The Viking Solar Corona Experiment

G. LEONARD TYLER

Stanford University, Stanford, California 94305

JOSEPH P. BRENKLE, THOMAS A. KOMAREK, AND ARTHUR I. ZYGIELBAUM

Jet Propulsion Laboratory, Pasadena, California 91103

The 1976 Mars solar conjunction resulted in complete occultations of the Viking spacecraft by the sun at solar minimum. During the conjunction period, coherent 3.5- and 13-cm wavelength radio waves from the orbiters passed through the solar corona and were received with the 64-m antennas of the NASA Deep Space Network. Data were obtained within at least 0.3 and 0.8 R_S of the photosphere at the 3.5- and 13-cm wavelengths, respectively. The data can be used to determine the plasma density integrated along the radio path, the velocity of density irregularities in the coronal plasma, and the spectrum of the density fluctuations in the plasma. Observations of integrated plasma density near the south pole of the sun generally agree with a model of the corona which has an 8:1 decrease in plasma density from the equator to the pole. Power spectra of the 3.5- and 13-cm signals at a heliocentric radial distance of about 2 R_S have a ½-power width of several hundred hertz and vary sharply with proximate geometric miss distance. Spectral broadening indicates a marked progressive increase in plasma irregularities with decreasing ray altitude at scales between about 1 and 100 km.

INTRODUCTION

The Viking mission and solar conjunction of Mars on November 25, 1976, provided a unique opportunity for studies of the K corona very near solar minimum. As Mars moved into and away from conjunction, the radio paths between the earth-based tracking station and Mars sliced through a region of the corona that included both equatorial and south polar solar latitudes. The observations extended from a heliocentric radial distance of 60 R_S (solar radii) to signal loss very near the photosphere. The coherent 3.5- and 13-cm (called X and S band) radio transmissions from the orbiters have been detected within at least 0.3 and 0.8 R_S of the photosphere, respectively. The regions through which the ray paths passed are particularly interesting, since they are thought to contain both the critical point (3–5 R_S), where coronal expansion goes from subsonic to supersonic flow, and the Alfvén point (5–10 R_S), where the magnetic and dynamic forces in the plasma are equal. These radio signals were received by the 64-m antennas of the NASA Deep Space Network in California and Australia. This paper discusses the observational factors involved and presents some very preliminary results.

Radio waves traversing the corona are affected in several ways: (1) they are deflected away from the sun by refraction, (2) the phase observed at the receiver is less, because the phase velocity is increased, but the time delay for a wave packet is greater, because group velocity is decreased, than would have been the case for signals propagating over the same path in the absence of the coronal electrons, and (3) the waves are scattered by turbulence in the corona so that there is partial randomization of amplitude and phase. All these effects are important in the Viking solar corona experiment, and since they are wavelength dependent, observation at two wavelengths permits a determination of the properties of the medium integrated along the radio path. The modulation time delay introduced by the corona is of the same sign as that of the time delay of general relativity, but the refraction is of opposite sign to that of the relativistic bending of light. Both are additionally of interest as corrections to the general relativity experiment utilizing the Viking landers [*Shapiro et al.*, 1977].

Observations of the radio propagation through the corona can be used to infer several fundamental quantities including the mean variation of coronal density with radial distance and the strength and structure of turbulence and/or waves in the coronal plasma. It may be possible to separate latitudinal and longitudinal effects on the basis of the variations in the geometry during the conjunction period.

The coronal medium has refractivity

$$\nu = -4.48 \times 10^{-16}\lambda^2 N_e \qquad (1)$$

where λ is the wavelength in meters, N_e is the electron number density per cubic meter, and the magnetic field and collisions are neglected. Absorption is negligible at the wavelengths of interest here. The refractive index $n = 1 + \nu$ is less than unity.

We have used the expression

$$N_e\left[\left(\frac{2.99}{\rho^{16}} + \frac{1.55}{\rho^6}\right) \times 10^{14} + \frac{3.44}{\rho^2} \times 10^{11}\right] \cdot(\cos^2\theta + \tfrac{1}{64}\sin^2\theta)^{1/2}\text{el}^-/\text{m}^3 \qquad (2)$$

where ρ is the distance (in solar radii) from the solar center of mass and θ is solar latitude, as a model of the corona. This model is the same as the Baumbach-Allen model [*Allen*, 1947; *Pottasch*, 1960] at the equator, where $\theta = 0$, except that we have added a latitudinal factor and a ρ^{-2} term corresponding to 7.5 el^-/cm^3 in the solar wind at the orbit of the earth. The latitudinal factor is heuristic; it approximates results from work on solar effects on radio observations of pulsars [*Weisberg et al.*, 1976]. This factor is an ellipse of axial ratio 8:1 and is of the same order as latitudinal variations determined from white light coronagraphs and eclipse observations near solar minimum. The value for the solar wind term was determined (by one of us, T.A.K.) from differential group delay measurements using Viking radio tracking prior to conjunction. It is in essential agreement with other similar determinations [*Brandt*, 1970; *Croft*, 1972].

The ρ^{-6} and ρ^{-2} terms are equal at just under 5 solar radii.

Paper number 7S0455.

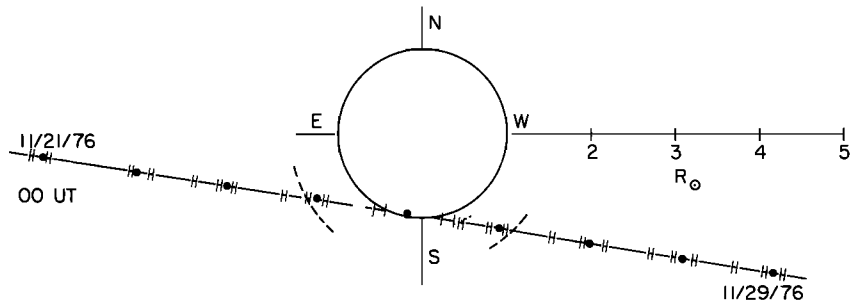

Fig. 1. Geometry of Viking solar corona observations and the geometric path of Mars in the plane of the sky for November 21–29, 1976. Bold points are positions at 0000 UT. The large circle represents the photosphere. Dotted and dashed segments are the geometric sizes of the 3.5- and 13-cm occulting disks, the limiting closest approach of the rays due to refraction, based on the same radial variation in plasma density as (2) in text, but with the latitudinal factor omitted. E-W directions are astronomic convention. Short hatch marks indicate positions where scintillation data were obtained. Farther from the sun the path of Mars is a smooth continuation of the curves shown. Data in Figure 2 are from E and W of this figure; data in Figures 5 and 6 are included in this figure.

This limit can be considered as defining a radio corona in terms of a rapid onset of propagation effects, but it should be noted that the solar plasma has a significant, often highly detrimental effect on radio propagation at the 13-cm wavelength as far out as 60–80 R_S.

Observations

Large- and Intermediate-Scale Coronal Structure

Differential dual-frequency measurements of apparent spacecraft range (time delay) and velocity (Doppler frequency) were used to determine the value and the time derivative, respectively, of the columnar electron content integrated along the propagation path. These values apply to a column with a cross-sectional area of Fresnel zone size, or about a 100-km diameter in the vicinity of the sun.

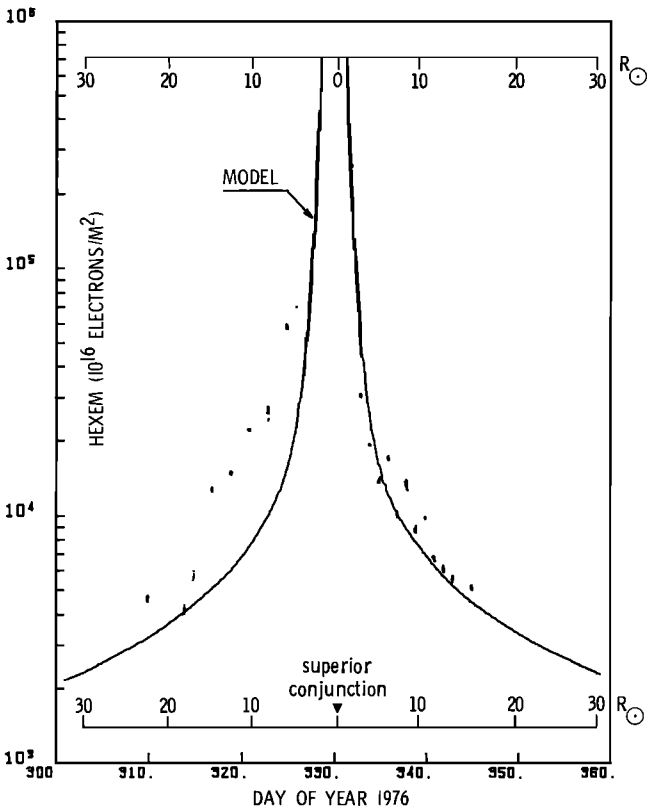

Fig. 2. Variation of measured columnar electron content of corona. The solid curve is a result of numerical integration of (2) in the text along geometric ray with closest approach A (see Figure 3) given by the inner scale. A total of 312 separate observations are included, many of which are indistinguishable at this scale. Note the strong asymmetry with respect to conjunction in both model and data. Day of year 330 is November 25, 1976.

The techniques employed have been discussed extensively elsewhere (for a discussion of the Viking system and operations, see *Michael et al.* [1972] and *Johnston et al.* [1977]). We note, however, that small changes in the total content are best determined when it is possible from the integral of the measured derivative with time and that the constant of integration is determined from the differential range. For observations within about 20 R_S, only the differential range was reliable because of the difficulties in accurate Doppler measurements under dynamic signal conditions.

Figure 1 depicts the geometric position of Mars with respect to the sun. The view is in the plane of the sky. The short intervals between small marks along the path indicate scintillation data coverage as explained in the caption. At distances greater than 5 R_S the path is a smooth continuation of the one shown. The coverage depicted here is only a fraction of the total but is all within 5 R_S of the sun's center.

Total electron content as determined from differential range measurements is given in Figure 2. The smooth curve in the figure corresponds to the modified Baumbach-Allen model of (2) above with the proper pole geometry included. The small groups of points in the figure are the result of independent range measurements on a single day. The standard error in these measurements is about 70×10^{16} el^-/m^2, so standard error bars in integrated content would not be visible in the presentation of Figure 2; the spread among points in a single day is the result of variations in the solar plasma with time. Figure 2 contains 312 separate observations, many of which overlie one another.

Most of the data presented for a single day in Figure 2 are based on differential range measurements using a device called the planetary ranging assembly (PRA) at the Australian 64-m antenna station. Unfortunately, this device had an ambiguity in the resolution of differential range of only 2 μs. This corresponds to an ambiguity in the integrated electron content of 8.456×10^{19} el^-/m^2. A different device, called the Mu-2 machine, with an ambiguity resolution of about 1 s, was in use at the California station. Mu-2 observations obtained just prior to the PRA observations were used to resolve the ambiguity associated with the use of the PRA alone. When the range residuals in tracking the Viking landers on the surface of Mars

are corrected for the effects of the plasma shown in Figure 2, they are typically much less than one-half the ambiguity in the PRA results, i.e., less than 1 μs; thus confidence in the results is increased. However, on isolated days, there are larger problems [see *Shapiro et al.*, 1977].

The model curve in Figure 2 is not symmetrical about the time of closest approach of the ray path to the center of the sun but is skewed leftward by the latitudinal factor in (2). Clearly, the measured values during the period just prior to conjunction exceed those predicted by the model by up to a factor of about 4. During the period immediately following conjunction the measured values and the model agree within a factor of less than 2 and are less than the values at the same distance from the sun prior to conjunction by a factor of about 5. Evidently, this rather strong change in integrated plasma density is indicative of pronounced variations along the ray path in the vicinity of the sun. The variations may be purely latitudinal, as is presumed in (2), or may represent a combination of latitudinal, temporal, and longitudinal effects.

Note that the increased plasma density observed prior to conjunction persisted for a time period of approximately 15 days. The measurements near the sun were effectively terminated by the effects of the corona prior to conjunction at about 5 R_S. Just after conjunction, differential range measurements were obtained as close as about 2 R_S, giving indirect evidence of asymmetry. In time these measurements corresponded to about one-half solar rotation following the maximum deviation from the model at about 10 R_S during occultation entry. Thus a purely longitudinal variation observed just before conjunction would have been carried across the path after conjunction by solar rotation. Further, no sunspots were observed in the southern hemisphere of the sun for 27 days prior to and for 18 days after occultation, although some calcium plagues were present. During all of November, only one small sunspot group appeared in the northern hemisphere near midmonth and disappeared over the western limb near the end of November [*National Oceanic and Atmospheric Administration*, 1976, 1977*a*, *b*]. While additional work on this point is required, the conditions of geometry and the lack of features on the photosphere are good preliminary evidence that the strong asymmetry observed is due to latitudinal variations similar to those in (2).

Velocity in the Coronal Plasma

For this discussion we need to distinguish between the motions of irregularities in the refractive index of the corona due to wave propagation through a particular region and those due to convective transport or mass flow. Radio methods are sensitive only to the motions of the refractive index fluctuations themselves, but these different events may have distinct signatures.

Under the frozen-in hypothesis for plasma it is expected that small fluctuations in the refractive index that occur outside the Alfvén point are carried along at the bulk velocity of the medium over some distance. Waves propagating through the medium are similarly translated by the large-scale motion. Near the sun the wave velocities and mass flow are thought to be of the same order, but at sufficiently small heliocentric distances the wave velocity is greater. The Viking measurements can be used to determine the velocities of coronal irregularities from cross correlation of the induced phase and intensity scintillations on two well-separated radio paths and from a characteristic feature in intensity scintillation spectra (see, for example, *Hewish* [1972], *Young* [1971], and *Jokipii* [1973]).

Velocity can be obtained rather directly by cross correlation of signals at the same wavelength over several Viking spacecraft-to-earth paths. These include signals transmitted from a single spacecraft to two earth stations and signals from two or more Viking spacecraft, usually an orbiter and a lander, received at the same ground station. The vector separation of the rays at the point of their closest approach to the sun is approximately 0.4 times the vector separation of the spacecraft in the plane of the sky. This separation is typically of the order of 10,000 km. If the lifetimes of smaller-scale irregularities are greater than the time to traverse this distance, about 30 s, then direct cross correlation of the signals will yield accurate velocities. Large-scale (100,000 km) irregularities persist much longer than 30 s [*Callahan*, 1975], but evidently, not much is known about lifetimes of irregularities at smaller scales. Radio astronomy observations of the solar wind suggest that the lifetime of a 100-km structure is greater than about 1 s, but there are suggestions that correlation over very large path separations may not be useful [*Dennison and Hewish*, 1967; *Hewish*, 1972]. If the lifetime of small-scale irregularities is too short to permit their use, we would hope to determine bulk velocity from such widely separated paths by searching for events associated with the passage of density gradients of material. The method of spaced receivers has been applied to observations of intensity scintillations of radio sources and tested by comparison with spacecraft data [*Jokipii*, 1973]. Simple theory gives agreement to within about 20%. More refined calculations improve the results.

We also expect to be able to use paths with much smaller separations to determine the radial component of velocity near the sun. Figure 3 schematically illustrates the geometry. Signals at the two wavelengths follow paths that are determined by the mean refractivity of the medium. The 3.5-cm wave undergoes the least bending, relative to which the 13-cm wave is always displaced toward the sun. The resulting ray path separation at ray perihelion is given in Figure 4. A disturbance moving radially outward from the sun will first perturb the 13-cm and then the 3.5-cm signal. The velocity would be determined by cross correlating simultaneous 3.5- and 13-cm wavelength observations of a single spacecraft by a single station. In the corona, where wave velocities may be typically 150 km/s at 2 R_S and the bulk velocities considerably less, the time delay will be of the order of seconds to tens of seconds, depending on the event and the geometry. Of additional interest, the magnitude of the correlation as a function of the vector path spacing is expected to be useful in weighting the plasma corrections for the Viking General Relativity experiment. Estimates of the coherency between the 3.5- and the 13-cm wavelength intensity, if no path separation is assumed, give values near 0.5

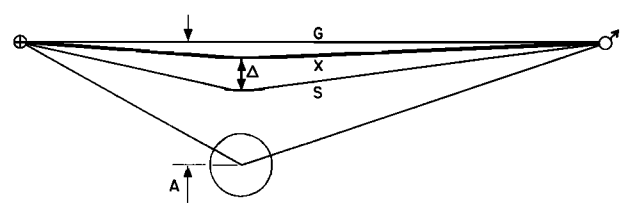

Fig. 3. Refraction of 3.5- and 13-cm waves in the corona and a schematic illustration of ray path bending due to coronal plasma. Paths are G, geometric ($\lambda = 0$); X, 3.5-cm; and S, 13-cm wavelengths. Distance A is closest approach of geometric ray, and distance Δ is ray path separation.

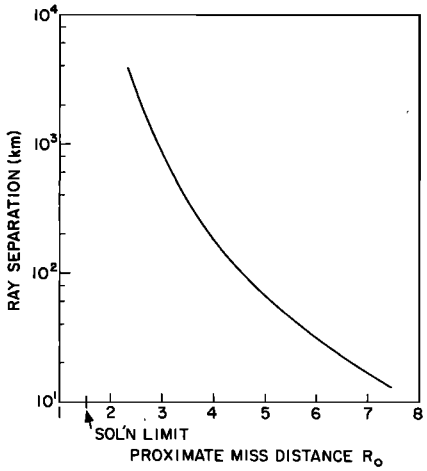

Fig. 4. Separation of 3.5- and 13-cm paths due to differential refraction. Ray path separation corresponds to distance Δ plotted versus distance A in Figure 3.

for this quantity [*Woo*, 1975]. This would be the approximate value of the cross correlation squared if the medium is perfectly rigid over the times required to traverse Δ in Figure 4.

The detectability of these effects based on the phase observable depends, as do the dual spacecraft observations, primarily on the short-term stabilities of the Viking spacecraft oscillators (about 1 part in 10^{10}). The passage of a plasma cloud of content equal to the earth's daytime ionosphere (10^{17} el^-/m^2) would correspond to a 10% fluctuation in plasma density at 5 R_S over a path length of about a 1/6 solar radius.

Finally, intensity scintillation spectra display a characteristic knee at a temporal frequency whose precise value depends on the geometry and distribution of the turbulence but is approximately the velocity divided by the Fresnel zone size. More specifically, this frequency is

$$f_F = ku/(\pi\lambda z)^{1/2}$$

where u is the velocity, z is approximately 1 AU, λ is the wavelength as before, the constant k is approximately unity, and the fluctuations of the medium are assumed to be isotropic [*Young*, 1971; *Jokipii*, 1973]. For plasma waves in the corona this frequency is of the order of 1 Hz and is easily observable in frequency spectra.

Because the Viking data offer several independent methods for determination of velocity, it will be possible to test the results for internal consistency and to test inferences based on the theory of scintillation against cross correlations of signals following different paths. Hopefully, it will be possible to separate events associated with wave phenomena from mass flow on the basis of theoretical considerations, ancillary observations, and event characteristics such as spectral shape.

Small-Scale Coronal Structure

The Viking coherent 3.5- and 13-cm radio systems are the first to provide direct occultation of the sun by coherent dual-frequency signals. Several previous spacecraft have provided observations at a single wavelength or, in the case of Mariner 10, which carried a similar coherent dual-frequency system, have not approached closer than about 7 R_S.

Most past radio astronomy and spacecraft studies of rapid (fluctuations faster than about 1 s) interplanetary or coronal scintillation have been restricted to fluctuations in signal intensity or apparent source size. These fluctuations are strongly coupled to variations in the refractive index of the medium that are approximately Fresnel zone size and smaller, or about 70 and 140 km for the 3.5- and 13-cm waves at solar distance. Viking dual-frequency spacecraft signals make it possible to observe rapid coronal scintillations in the phase of the signals as well. (Differential phase measurements or their equivalent have been made by numerous others; they have been specifically interpreted as large-scale scintillations by *Callahan* [1975] and *Woo et al.* [1976].) Differential phase scintillations are sensitive to refractive index fluctuations over all scales significantly greater than the tracking station antenna size, a lower bound that is shared with the effects of the medium on intensity fluctuations. Thus conservatively, the Viking data contain information on all scales in the corona greater than about 1 km without the need to consider the effects of finite antenna beam width. The problem of extracting scale size information from the observed intensity and phase scintillations is straightforward, since the relationship between the turbulence spectrum and the scintillations is known (see, for example, *Jokipii* [1973]).

Here we present examples of spectral broadening observed during the Viking conjunction period. Figure 5 shows the power spectra of the received signals at three different times during the experiment. The data shown were all taken by using

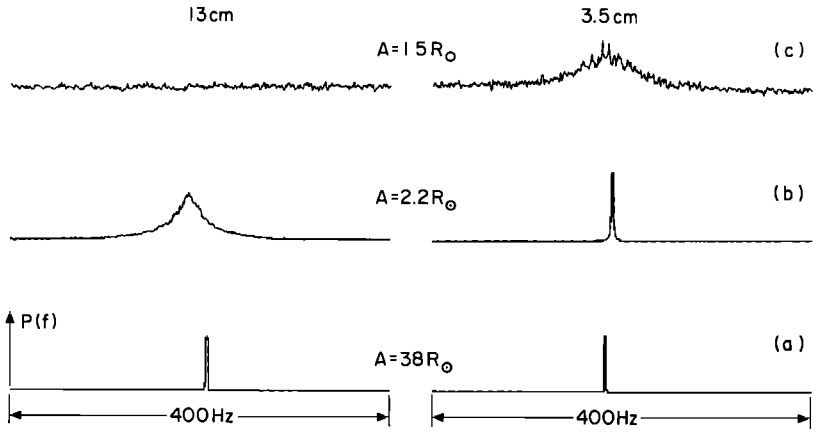

Fig. 5. Spectral broadening of 3.5- and 13-cm waves. Sequence of power spectra for three geometric positions of earth, sun, and Mars are characterized by closest approach of geometric ray path A (see Figure 3). Absence of the 13-cm signal in 5*c* is due to corona. A spurious signal, 0.2 intensity of the 3.5-cm wave, about 50 Hz higher in frequency than that of the 3.5-cm wave, has been deleted from the Figure 5*b* 3.5-cm data.

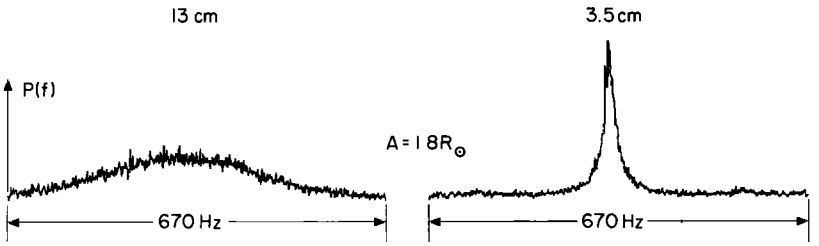

FIG. 6. Simultaneous 3.5- and 13-cm spectral broadening at 1.8 R_S. There is well-developed spectral broadening near the limit of the 13-cm penetration. A spurious signal has been deleted from the center of the 13-cm spectrum; otherwise spectra are as computed. Leftward skew of the 13-cm signal is apparently real but needs further study. These spectra were obtained 5 hours before those of Figure 5*c*.

the spacecraft auxiliary oscillator as a frequency reference for the spacecraft. On the time scale of these observations, about 200 s, the spectral width of the transmitted signal is near 1 and 4 Hz at the 13- and 3.5-cm wavelengths, respectively. Figure 5*a* is typical of ray paths that miss the coronal region but are still influenced by the interplanetary medium. Power spectral density is plotted linearly, and the horizontal axes of both the 3.5- and the 13-cm wavelength signal are the same, 400 Hz full width. The signals, which appear near the center of the plots in Figure 5*a*, show slight spectral broadening at 13 cm and less at 3.5 cm. Figures 5*b* and 5*c* show progressive effects of propagation in deeper portions of the corona. In Figure 5*b* the 13-cm wavelength is significantly affected, but on the scales shown, the 3.5-cm signal shows no significant effects. In Figure 5*c*, which corresponds to a ray path near the theoretical 13-cm occulting disk (the limiting distance of closest approach based on refraction, see Figure 1), the 13-cm signal has degraded to the point where it is no longer apparent. Note that the transition from Figure 5*b* to Figure 5*c* is very rapid owing to the ρ^{-6} dependence in coronal structure. The 3.5-cm signal is still readily detectable in spectra such as these when the ray path is 1.3 R_S from the center of the sun.

An intermediate condition to Figures 5*b* and 5*c* is illustrated in Figure 6, in which there is marked spectral broadening at both wavelengths. Note that the horizontal scale in Figure 6 has been expanded. The conditions of Figure 6, which occurred at about 1.8 R_S, or only slightly outside the conditions of Figure 5*c*, lasted only a few hours.

In the broadened scintillation spectra the shift in frequency from the undisturbed (by the irregularities) position is directly related to the velocity of irregularities u and the vector component of wave number of the plasma irregularity in the direction of the velocity k_u. The frequency offset is then $uk_u/2\pi$, independent of the radio wavelength. If 200 km/s represents a typical plasma bulk velocity high in the corona, then the frequency displacements easily visible in Figure 6 represent the effects of structure down to about 2 km in size.

APPLICATIONS

Independent measures of coronal plasma density, velocity, and structure larger than about 1 km in scale make it possible to determine (1) the distribution of coronal plasma, (2) the velocity of irregularities in the corona and probably the mass flow, and (3) the spectrum of the turbulence down to scales as small as about 1 km. The geometry of the Viking experiment permits comparison of equatorial and south polar regions as given by the example of the integrated plasma content above.

One problem of particular interest is that of regions of relatively low X ray, UV, and radio emissivity (and therefore relatively low temperature and/or density) in the corona, called 'coronal holes.' Coronal holes are observed to be the source of high-speed solar wind streams having relatively high particle fluxes [*Nolte et al.*, 1976]. To account for the apparent contradiction between this source's behavior and its being a region of low density and/or temperature, *Kopp and Holzer* [1976] and others have suggested that the critical point in coronal expansion is located much closer to the sun ($\lesssim 2\ R_S$) in coronal holes than it is elsewhere. Thus the flow becomes supersonic low in the corona and remains supersonic at larger heliocentric distances. We hope to test this hypothesis experimentally. Because the ray path trajectory passes through the southern polar corona before and after occultation, it provides an opportunity to study one such region continuously located above the sun's polar latitudes at solar minimum. It has also been suggested [*Jackson*, 1977] that there is significant energy deposition beyond 3 R_S, far above the base of the corona. Since the radio link data are a measure of wave and shock disturbances, on a time scale greater than that required to form a reliable spectrum, about 1 s, energy deposition by these means can be investigated.

Disturbances in the solar wind observed near 1 AU such as shocks and magnetohydrodynamic waves are often assumed to originate in the low corona [*Hundhausen*, 1972; *Wu et al.*, 1976]. Such disturbances in the low corona are presumably detectable by the Viking radio link experiment, although the ray path trajectory made near-ecliptic measurements possible only at relatively large distances from the sun ($\gtrsim 3\ R_S$). The measurement of events both in the low corona and in the interplanetary medium is expected to be useful in evaluating theoretical work on disturbance propagation in the solar wind (for example, that of *Hundhausen and Gentry* [1969] and *Wu et al.* [1976]).

The fact that the occultation took place very near solar minimum provides a considerable advantage. First, the flow structure of the corona was in its most simple state, relatively undisturbed by active regions. Second, studies of the corona above active regions will be relatively simple. That is, there were very few active regions on the sun at this time, and thus studies of the corona above an individual active region (for example, using the radio link data in conjunction with ground-based and spacecraft data from Oso 8 and Helios 1 and 2) are not subject to confusing effects from nearby active regions as would likely be the case at times of more solar activity. Further, the data will be extremely interesting for comparison with similar observations at the same wavelengths from Mariner 10, which passed about 7 R_S over the north pole of the sun in 1974, and from Voyager during the next solar maximum.

CONCLUSIONS

Viking 3.5- and 13-cm radio data penetrated the solar corona to very near the limits expected on the basis of previous optical studies. The measured columnar electron content is

strongly asymmetric in terms of radial dependence with respect to conjunction. This asymmetry reflects either a strong latitudinal dependence of coronal plasma density or a latitudinal dependence in combination with other variations. Spectral broadening of the signals penetrating the corona indicates a marked progressive increase in plasma irregularities with decreasing distance from the sun at scales greater than about 1 km. The data are not yet completely reduced; these results are based on the first preliminary analyses of the observations.

Acknowledgments. The authors gratefully acknowledge the assistance and support of the Viking Project staff and especially their colleagues on the Viking Radio Science Team. We also note many useful discussions with J. F. Vesecky and the efforts of B. Seidel in the collection of the scintillation data. This work at Stanford and at the Jet Propulsion Laboratory was carried out as a part of the NASA Viking mission by using the facilities of the NASA Deep Space Network but also depended in part on ongoing NASA programs in the use of radio propagation data at both institutions. NASA contract NAS1-9701.

REFERENCES

Allen, C. W., Interpretation of electron densities from corona brightness, *Mon. Notic. Roy. Astron. Soc., 107,* 426–432, 1947.

Brandt, J. C., *Introduction to Solar Wind,* W. H. Freeman, San Francisco, Calif., 1970.

Callahan, P. S., Columnar content measurements of the solar-wind turbulence near the sun, *Astrophys. J., 199,* 227–236, 1975.

Croft, T. A., Solar wind concentration averaged in time and space (abstract), *Eos Trans. AGU, 53,* 505, 1972.

Dennison, P. A., and A. Hewish, The solar wind outside the plane of the ecliptic, *Nature, 213*(5074), 343–346, 1967.

Hewish, H., Observations of solar plasma using radio scattering and scintillation methods, Solar Wind, *NASA Spec. Publ., 308,* 477–493, 1972.

Hundhausen, A. J., *Solar Wind and Coronal Expansion,* Springer, New York, 1972

Hundhausen, A. J., and R. A. Gentry, Numerical simulation of flare-generated disturbances in the solar wind, *J. Geophys. Res., 74*(11), 2908, 1969.

Jackson, B. V., A coronal hole equatorial extension and its relation to a high speed solar wind stream, paper presented at Topical Conference on Solar and Interplanetary Physics, AGU and Amer. Astron. Soc., Tucson, Ariz., Jan. 12–15, 1977.

Johnston, D. W., T. W. Howe, G. M. Rockwell, Viking mission support, *Progr. Rep. 42–37,* pp. 12–25, Deep Space Network, Jet Propul. Lab., Pasadena, Calif., 1977.

Jokipii, J. R., Turbulence and scintillations in the interplanetary plasma, in *Annu. Rev. Astron. Astrophys., 11,* 1–28, 1973.

Kopp, R. A., and T. E. Holzer, Dynamics of coronal hole regions, I, Steady polytropic flows with multiple critical points, *Solar Phys., 49,* 43–56, 1976.

Michael, W. H., Jr., D. L. Cain, G. Fjeldbo, G. S. Levy, J. G. Davies, M. D. Grossi, I. I. Shapiro, and G. L. Tyler, Radio science experiments: The Viking Mars orbiter and lander, *Icarus, 16,* 57–73, 1972.

National Oceanic and Atmospheric Administration, Solar geophysical data prompt report, I, *Rep. 388,* U.S. Dep. of Commer., Boulder, Colo., Dec. 1976.

National Oceanic and Atmospheric Administration, Solar geophysical data prompt report, I, *Rep. 389,* U.S. Dep. of Commer., Boulder, Colo., Jan. 1977*a*.

National Oceanic and Atmospheric Administration, Solar geophysical data prompt report, I, *Rep. 390,* U.S. Dep. of Commer., Boulder, Colo., Feb. 1977*b*.

Nolte, J. T., A. S. Krieger, A. F. Timothy, R. E. Gold, E. C. Roelof, G. Viana, A. J. Lazarus, J. D. Sullivan, and P. S. McIntosh, Coronal holes as sources of the solar wind, *Rep. ASE-3817,* Amer. Sci. and Eng., Cambridge, Mass., 1976.

Pottasch, S. R., Use of the equation of hydrostatic equilibrium in determining the temperature distribution in the outer solar atmosphere, *Astrophys. J., 131,* 68–74, 1960.

Shapiro, I. I., R. D. Reasenberg, P. E. MacNeil, R. B. Goldstein, J. P. Brenkle, D. L. Cain, T. A. Komarek, A. Zygielbaum, W. F. Cuddihy, and W. H. Michael, Jr., The Viking relativity experiment, *J. Geophys. Res., 82,* this issue, 1977.

Weisberg, J. M., J. M. Rankin, R. R. Payne, and C. C. Counselman III, Further changes in the distribution of density and radio scattering in the solar corona in 1973, *Astrophys. J., 209,* 252–258, 1976.

Woo, R., Multifrequency techniques for studying interplanetary scintillations, *Astrophys. J., 201,* 238–248, 1975.

Woo, R., F. C. Yang, K. W. Yip, and W. B. Kendall, Measurements of large scale density fluctuations in the solar wind using dual-frequency phase scintillations, *Astrophys. J., 210*(2), part I, 568–574, 1976.

Wu, S. T., M. Dryer, and S. M. Han, Interplanetary disturbances in the solar wind produced by density, temperature or velocity pulses at 0.08 A.U., *Solar Phys., 49,* 187–204, 1976.

Young, A. T., Interpretation of interplanetary scintillations, *Astrophys. J., 168,* 543–562, 1971.

(Received March 31, 1977;
revised May 23, 1977;
accepted May 25, 1977.)